

Concave Wall Heat Transfer Characteristics with Longitudinal Pressure Gradients and Discrete Wall Jets*

Habib UMUR**

The effects of free stream velocities, longitudinal pressure gradients and discrete wall jets on concave wall heat transfer characteristics have been examined in wind tunnel and water channel flows at momentum thickness Görtler numbers from 5 to 30 at the initial station. It was shown that longitudinal vortices became suppressed with increasing free stream velocities. The pressure gradient parameters of up to 0.75×10^{-6} resulted in a regular vortex structure and caused mean heat transfer coefficient to increase. The pressure gradient parameter of 1.8×10^{-6} was sufficient to suppress the vortex development so that there was no heat transfer augmentation above that of flat plate values. Measurements with blowing parameters of up to unity showed that the streamwise vortices and the wall temperature patterns were controlled by the jets so that maximum Stanton numbers exceeded minimum values by a factor of around three. With blowing parameters larger than unity, the interaction between the streamwise vortices and the wall jets caused irregularities in wall temperature patterns so that the streamwise variation of Stanton number remained nearly unchanged.

Key Words: Concave Surface, Longitudinal Vortices, Pressure Gradients, Discrete Wall Jets, Heat Transfer Enhancement

1. Introduction

Longitudinal concave curvature can cause boundary layer instability which stems from amplification of small disturbances, and can form a counterrotating vortex system, the so-called Görtler vortices. It has long been recognised that streamwise vortices can account for high heat transfer rates in practice, so that most studies with concave curvature so far have been concentrated on the effects of streamwise vortices on wall heat transfer variations. For instance, McCormack et al.⁽¹⁾ demonstrated an increase in Nusselt number by a factor of around two, with a Görtler vortex system on a concave wall, compared with that on a flat wall. Kelleher et al.⁽²⁾ reported a nearly threefold increase in Stanton number with a secondary-flow structure similar to a Görtler vortex system, and the more recent measurements of Kottke⁽³⁾ on a curved plate, with a range of grids,

appear to show that the extent of heat transfer enhancement depends on the intensity of turbulence in the upstream flow and on its scale relative to the Görtler vortex wavelength. Crane and Umur⁽⁴⁾ showed that the enhancement in Stanton number was delayed until Görtler number reached around 10. On the other hand, an increase of 20% in Stanton number due to concave surface curvature and without any apparent vortex structure was observed by Thomann⁽⁵⁾, and a similar increase by Mayle et al.⁽⁶⁾ and by Simonich and Moffat⁽⁷⁾. In contrast, the Stanton number on a surface of the convex curvature decreased by 15, 20 and 20% according to the results of Thomann⁽⁵⁾, Mayle et al.⁽⁶⁾ and Gibson et al.⁽⁸⁾, respectively. The flows in these last three experiments were turbulent so that longitudinal vortices could not be identified. There have been a small number of investigations of the effects of discrete wall jets on heat transfer. Hartnett et al.⁽⁹⁾ reported that discrete wall jets caused a slight increase in Stanton number and Ligrani et al.⁽¹⁰⁾ showed that Stanton number increased more rapidly with downstream distance for a blowing parameter of 0.47 than of near unity. More recently, Crane and Umur⁽¹¹⁾ reported that the effect of discrete

* Received 22nd September, 1992.

** Mechanical Engineering Department, Engineering and Architecture Faculty, Uludag University, 16059, Bursa, Turkey

hole injection on vortex structure was dependent on the magnitude of the blowing parameter.

The present experiments have been carried out in two rigs to investigate the heat transfer characteristics under the influence of the concave curvature with favourable pressure gradients in air, and with discrete wall injection into a main stream in water.

2. Flow Configurations

The low-speed wind tunnel of Fig. 1 was used, with an area contraction ratio of nine and with a working section with entrance-plane dimensions of 127 mm in height and 762 mm in width. The free stream velocity and turbulence intensity at the exit from the contraction were 5 m/s and 0.2%, respectively, and the flow was free of swirl and symmetric with boundary layer thickness on the order of 9 mm. Experiments were performed with an adjustable test section of 1 250 mm in length and with and without effective longitudinal pressure gradient [$k = (\nu/u^2)(du/dx)$]. The velocity measurements were previously recorded and published, and then wall-temperature variations were measured with a liquid crystal arrangement described by Umur⁽¹²⁾.

The water channel flow configuration Fig. 2(a) was also used to investigate the combined effects of longitudinal vortices and discrete-hole wall jets with pitch similar to that associated with the vortices on heat transfer characteristics. Velocity measurements were recorded in advance by laser Doppler velocimetry and wall temperatures, again by liquid

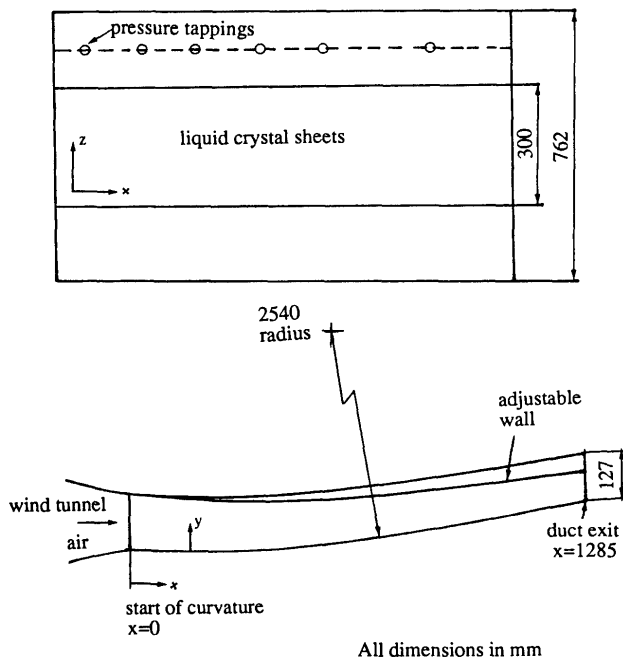


Fig. 1 Wind tunnel test section and location of instrumentation

crystals. The test section comprised a 90-degree bend with a radius of concave curvature of 140 mm and a cross section of 40x200 mm. In this case, the free stream velocity at the entrance to the working section was 0.12 m/s and the turbulence intensity was again less than 0.01. The discrete jets of Fig. 2(b) were injected through 2.5-mm-diameter holes with a pitch of 10 mm and aligned at an angle of 60 degrees to the curved wall. The average velocity through each hole was 0.048 to 0.378 m/s and the free stream velocity was varied from 0.12 to 0.252 m/s to provide velocity ratios (m) from zero to 1.5.

The purpose of the experiments was to define the effects of longitudinal vortices, in a range of Görtler number [$G_\theta = (u\theta/\nu)\sqrt{\theta/R}$] up to 30, on heat transfer characteristics under the influence of favourable pressure gradients and discrete wall jets.

3. Results and Discussion

The following results correspond to Stanton number variations measured with initial free stream velocities of 5, 10 and 15 m/s on the curved surface and with the three favourable pressure gradients corresponding to k of 0.2, 0.75 and 1.8×10^{-6} in the wind tunnel and

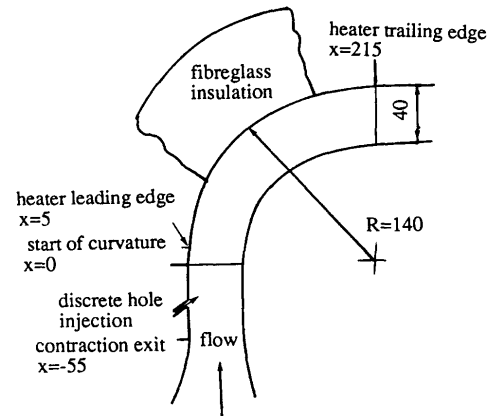


Fig. 2(a) Water channel test section with liquid crystal and heater geometry

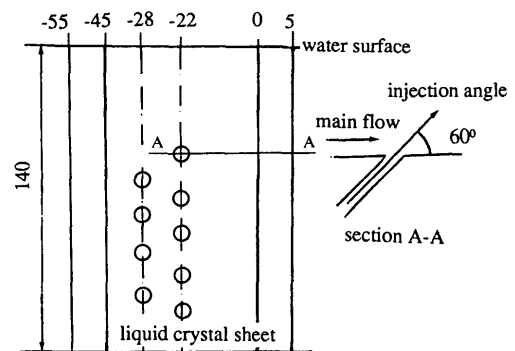


Fig. 2(b) Discrete hole injection geometry

with initial free stream velocities of 0.120 and 0.252 m/s with injection ratios (m) of 0.0, 0.4, 1.0 and 1.5 in the water channel.

3.1 Flow with zero pressure gradient

The investigation was carried out with core flow velocities of 5, 10 and 15 m/s in the plane of the contraction and therefore in the plane of the entrance of the present curved duct. Wall temperatures have been measured on the concave wall with the liquid crystal sheet described by Umur⁽¹²⁾. An example of the wall temperature distribution is shown in Fig. 3 with the corresponding temperature and Stanton number distributions at the locations $Re_x \approx 0.38 \times 10^6$ and $Re_x \approx 0.43 \times 10^6$. The heat transfer coefficient is defined as $h = q / (T_w - T_\infty)$ where, T_w , T_∞ and q are the wall temperature, free stream temperature and heat flux, respectively. It is presented in the form of a Stanton number, defined as

$$St = h / (\rho u_\infty C_p), \tag{1}$$

where ρ , u_∞ and C_p are the density of fluid, the free stream velocity and the constant pressure specific heat of the fluid. In these measurements, the local temperature was obtained by varying the heat flux until a particular colour was observed, so that the boundary condition corresponded to a constant heat flux and a constant temperature, but at different times. Thus, theoretical results are presented for laminar flow with constant temperature and constant heat flux together

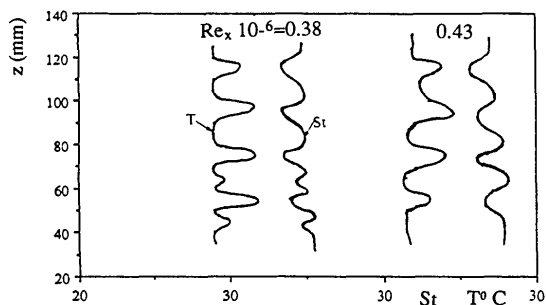


Fig. 3 Wall temperature and Stanton number distributions

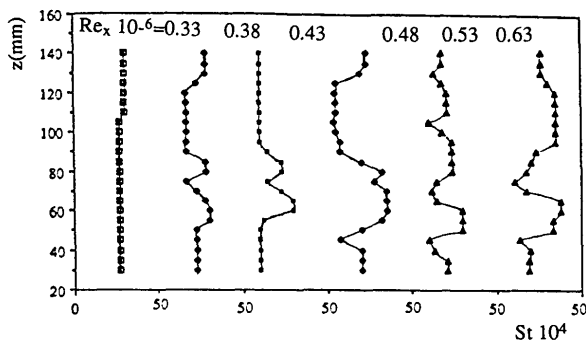


Fig. 4 Spanwise variation of Stanton number at $u = 5$ m/s

with a correlation for turbulent flow which is applicable to both boundary conditions.

Stanton numbers of Fig. 4 with the free stream velocity of 5 m/s indicate a wavelength of 20 mm at $Re_x = 0.53 \times 10^6$. These results are also shown in Fig. 5, where the maximum and minimum values may be compared with correlation formulae

$$St = B Re_x^{-0.5} Pr^{-2/3} [1 - (x_1/x)^{0.75}]^{-1/3} \tag{2}$$

$$St = B Re_x^{-0.2} Pr^{-0.4} [1 - (x_1/x)^{0.9}]^{-1/9} \tag{3}$$

for laminar and turbulent flow on a flat plate, where x is distance from the virtual origin and x_1 is the unheated starting length which is constant during a measurement. Re_x is the Reynolds number based on distance from an effective boundary layer origin determined from a measured velocity profile at $x = 100$ mm. B has the value of 0.332 for constant wall temperature T_w and 0.453 for constant heat flux Q_w in laminar flow and 0.03 for turbulent flow with either boundary condition⁽¹³⁾.

The spanwise averaged Stanton number for zero pressure gradient decreases until the Görtler number reaches 10 for $Re_x = 0.43 \times 10^6$, then increases with streamwise distance. The values of mean Stanton numbers are above those for a laminar flat plate over all the surface and exceed the turbulent values for $Re_x = 0.63 \times 10^6$. The mean value of St is twice that of the laminar flat plate solution for $Re_x = 0.48$ and 0.53×10^6 . The increase in heat transfer with concave curvature is consistent with the findings of McCormack et al.⁽¹⁾, who experimentally investigated the effect of streamline curvature on heat transfer in laminar flow, and Kelleher et al.⁽²⁾, who showed an increase of almost 200% on the outer wall of a curved rectangular channel with a secondary flow structure similar to a Görtler vortex system. The maximum (downwash) St is almost three times greater than the minimum in the chosen vortex pair. The local increase in St at downwash locations, where the cold fluid is swept to the wall, can be attributed to the thinner boundary layer (see Fig. 5) and the effects of cross-flow.

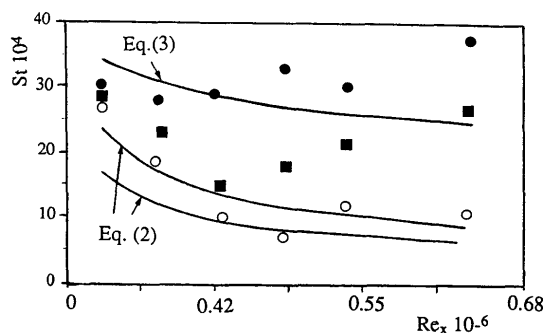


Fig. 5 Experimental Stanton numbers and values for Eqs. (2) and (3); ●: downwash, ○: upwash, ■: mean Stanton number

A simple empirical relationship for enhancement of laminar heat transfer by Görtler vorticity was proposed by Kan et al.⁽¹⁴⁾, based on one set of measurements of mass transfer from a naphthalene-coated blade in a turbine cascade. They correlated the ratio of measured values to flat plate values

$$St_{con}/St_{flat}=(1+G_{\theta})^{1/2} \quad (4)$$

This empirical relationship, as seen in Fig. 6, overestimates the heat transfer enhancement of the present results for much of the surface and shows a sudden increase in heat transfer for the nonzero Görtler number at the start of the curvature, because it takes no account of precurvature boundary layer development. Eq. (4) was modified to give unity at the beginning of the curvature,

$$St_{con}/St_{flat}=(1+G_{\theta,l}-G_{\theta,s})^{1/2} \quad (5)$$

with $G_{\theta,l}$ being the local Görtler number at any location and $G_{\theta,s}$ the Görtler number at the beginning of the curvature. Equation 5 is shown, in Fig. 6, to be in better agreement with the measurements than the unmodified flat-plate analytical solution and Eq. (4), but it does not reproduce the rising trends in the measured $St(x)$ distributions, and it is likely that no single function of G_{θ} can adequately model data from more than one flow facility, because of the difference in disturbance strength at the onset of curvature.

Figure 7 shows that the amplification of spanwise

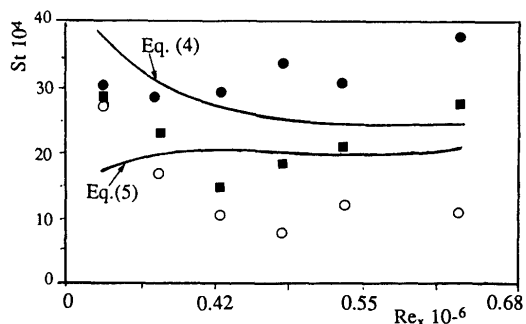


Fig. 6 Experimental Stanton numbers and values for Eqs. (4) and (5); ● : downwash, ○ : upwash, ■ : mean Stanton number

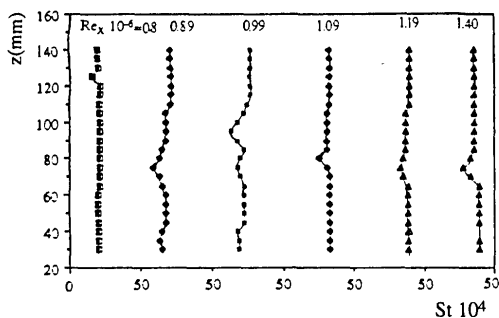


Fig. 7 Spanwise variation of Stanton number at $u=10$ m/s

variation of Stanton numbers at $u=10$ m/s is almost negligible and Fig. 8 shows that the spanwise averaged Stanton number is always larger than the laminar values and larger than turbulent values at $Re_x \geq 1.09 \times 10^6$. The rise in Stanton number with Re_x may be the result of boundary layer transition, with little influence from longitudinal vortices. The spanwise variations of Stanton number and the spanwise averaged Stanton numbers at 15 m/s are the same as at 10 m/s. The spanwise averaged Stanton numbers exceed the turbulent values by a factor of 1.4 towards the end of curvature. In the work of Thomann⁽⁵⁾, wall heat transfer in a supersonic flow ($Ma=2.5$) turbulent boundary layer was increased by about 20% on a concave surface, and decreased by about 15% on a convex surface. Mayle et al.⁽⁶⁾ found that heat transfer in a turbulent wall flow increased 33% on the concave side and decreased 20% on the convex side. Gibson et al.⁽⁸⁾ showed that Stanton number fell by 18% from the predicted flat plate value on a mildly curved convex surface, but the flows were fully developed and without Görtler vortices, so the heat transfer enhancement resulted from the curved surface and the corresponding body force.

Temperature and heat flux measurements were also made with 2-mm-high and 20-mm-wavelength vortex generators and led to the spanwise distributions of Stanton number, as shown in Fig. 9, and are consistent with the work of Kamotoni et al.⁽¹⁵⁾, who reported that the wavelength of the vortices remained unchanged with heating, although the strength was enhanced. The amplitude of spanwise Stanton number was found to grow with streamwise distance until $Re_x=0.53 \times 10^6$, where highly inflected velocity profiles occurred. The growth rate depended on the stage of amplification of the particular vortex pair, and Fig. 10 shows a plot of the variation of maximum and minimum measured values of Stanton number with Reynolds number and the flat plate correlations. The spanwise averaged Stanton number again decreased

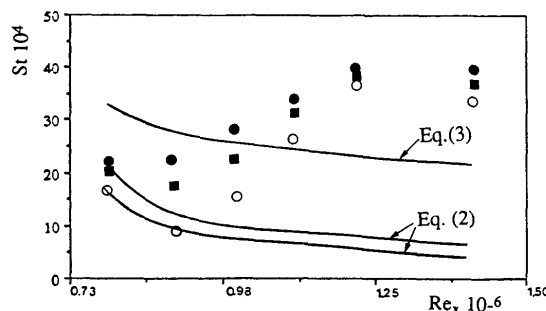


Fig. 8 Experimental Stanton numbers and flat plate values at $u=10$ m/s; ● : downwash, ○ : upwash, ■ : mean Stanton number

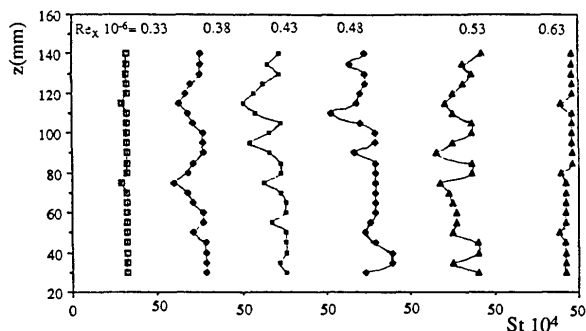


Fig. 9 Spanwise variation of Stanton number with vortex generator; $h=2$ mm, $\lambda=20$ mm and $u=5$ m/s

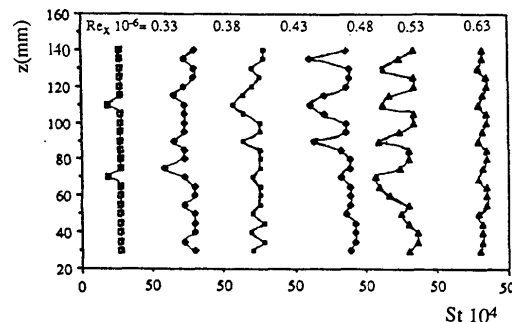


Fig. 11 Spanwise variation of Stanton number at $u=5$ m/s and $k=0.2 \times 10^{-6}$

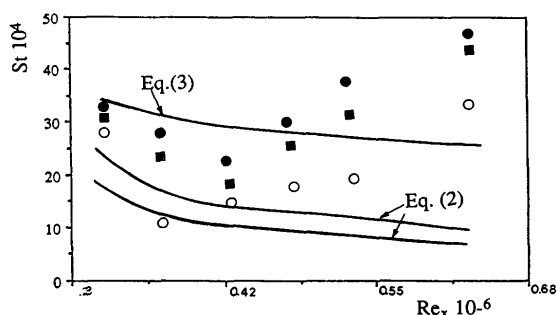


Fig. 10 Experimental Stanton numbers and flat plate values at $u=5$ m/s with vortex generator, $h=2$ mm and $\lambda=20$ mm; \bullet : downwash, \circ : upwash, \blacksquare : mean Stanton number

up to a Görtler number of 10, where $Re_x=0.43 \times 10^6$, then increased with streamwise distance. The heat transfer appears to have been enhanced by the vortex system, rising to levels comparable with turbulent correlations at $Re_x \geq 0.48 \times 10^6$. The amplitude of spanwise variation of Stanton number is around 50% of the spanwise mean value, which is twice that of the laminar flat plate correlation at $Re_x=0.43$ and 0.58×10^6 , where $G_\theta \geq 10$ and inflected velocity profiles were present. These results are consistent with those of McCormack et al.⁽¹⁾, but larger than those of Kottke⁽³⁾, who reported that the extent of heat transfer enhancement (up to 80%) depended on the intensity of turbulence in the upstream flow and on its scale relative to the Görtler vortex wavelength. The maximum Stanton number in a vortex pair is seen to exceed the turbulent flat-plate level, and the minimum, St , to exceed that of the laminar flat-plate values at $Re_x \geq 0.48 \times 10^6$. The maximum value of Stanton number is more than twice the minimum value. Crane and Sabzvari⁽¹⁶⁾ showed that the reduced boundary layer thickness alone could account for some 60% of the difference between the measured value of the spanwise averaged Stanton number and that for laminar flow, so that the local increase in heat transfer can be attributed to the three-dimensional

behaviour of the vortex system, rather than to the result of reduced boundary layer thickness in downwash zones.

3.2 Flow with favourable pressure gradients

Heat transfer measurements were also made using favourable pressure gradients of 0.2, 0.75 and 1.8×10^{-6} so as to determine the influence of acceleration on heat transfer and, in this case, Eqs. (4) and (5) are not appropriate, so Young's method and Reynolds analogy, corrected for the unheated starting length, were preferred for the comparison. The Stanton number for laminar boundary layer flows with pressure gradient may be written as

$$St = (C_f/2) Pr^{-2/3} [1 - (x_1/x)^{0.75}]^{-1/3}, \quad (6)$$

where

$$C_f = (2\nu/9u\theta)(2 + \lambda_1/6)$$

and

$$\lambda_1 = (\delta^2/2) du/dx.$$

At $k=0.2 \times 10^{-6}$, the spanwise distribution of Stanton number in Fig. 11 shows a greater amplitude, up to 45% of the spanwise mean value, than those of the near-zero pressure gradient flow. The small acceleration factor of 0.2×10^{-6} , which stabilised the boundary layer development and gave rise to more regular vortex structure, resulted in higher spanwise averaged Stanton numbers than with near-zero pressure gradient, as shown in Fig. 12, which also compares the maximum, minimum and mean Stanton numbers with Eqs. (2), (3) and (6). While the minimum Stanton number remains close to the laminar correlations the maximum Stanton number starts from a laminar value and exceeds a turbulent one for $Re_x \geq 0.48 \times 10^6$. The results at $Re_x \geq 0.63 \times 10^6$ ($x=1050$ mm) should be treated cautiously, because of the possible influence of the open downstream edge of the test section. The maximum Stanton numbers in the chosen vortex pair ($z=80$ mm to 100 mm) exceeded those at upwash values by a factor of 1.5 at $Re_x=0.33 \times 10^6$ and 3.5 at $Re_x=0.48 \times 10^6$, where the vortices were very strong. The streamwise variation of spanwise averaged Stanton number started from

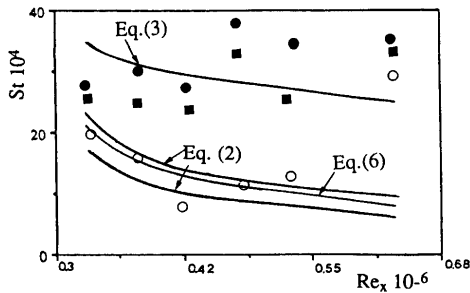


Fig. 12 Experimental Stanton numbers and flat plate values at $u=5$ m/s and $k=0.2 \times 10^{-6}$; ● : downwash, ○ : upwash, ■ : mean Stanton number

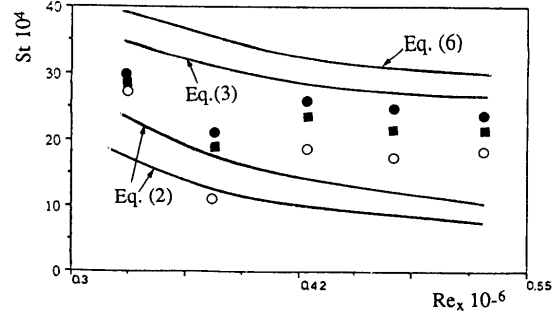


Fig. 14 Experimental Stanton numbers and flat plate values at $u=5$ m/s and $k=1.8 \times 10^{-6}$; ● : downwash, ○ : upwash, ■ : mean Stanton number

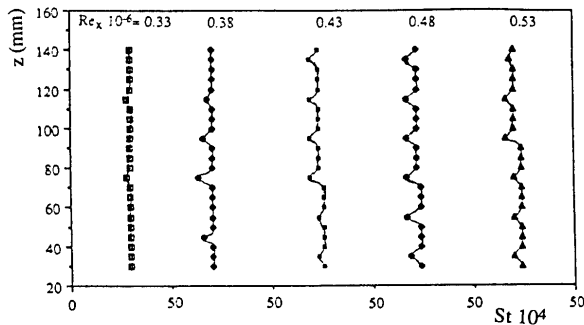


Fig. 13 Spanwise variation of Stanton number at $u=5$ m/s and $k=1.8 \times 10^{-6}$; ● : downwash, ○ : upwash, ■ : mean Stanton number

27×10^{-4} at $Re_x=0.33 \times 10^6$, decreased only slightly at $Re_x=0.43 \times 10^6$ until a Görtler number of 10 was reached, and then increased. At $Re_x=0.48 \times 10^6$ where the vortex system became strongest, the Stanton number reached a peak value of 33×10^{-4} , which may be attributed to the positive effects of longitudinal Görtler vortices and accelerating core flows.

The spanwise distributions of Stanton number for $k=0.75 \times 10^{-6}$ are similar to $k=0.2 \times 10^{-6}$, having the broad, flattened crests of downwash regions and narrow troughs of upwash regions. The amplitude of the spanwise variation of Stanton number is around 45% of the spanwise mean value. The spanwise averaged Stanton numbers decreased until $Re_x=0.43 \times 10^6$ and then increased, with values similar to those with streamwise curvature corresponding to $k=0.2 \times 10^{-6}$. The increase in heat transfer with the acceleration factor is consistent with the work of Junkhan and Serovy⁽¹⁷⁾, who showed that acceleration caused heat transfer to increase in laminar boundary layers but not in turbulent boundary layers.

The spanwise distribution of Stanton numbers for $k=1.8 \times 10^{-6}$ (Fig. 13) shows smaller amplitudes of spanwise distribution of Stanton number, 20% of the spanwise mean value. The maximum and minimum Stanton numbers are close to each other near the

downstream edge and throughout the concave surface. The spanwise averaged Stanton numbers of Fig. 14 decreased until $Re_x=0.38 \times 10^6$, then increased slightly at the subsequent stations, remaining below the values determined by Eq. (6). The experimental results show that heat transfer increased with acceleration for $k=0.2 \times 10^{-6}$ and $k=0.75 \times 10^{-6}$ but decreased at $k=1.8 \times 10^{-6}$, which was sufficient to suppress and weaken the vortices.

3.3 Flow with discrete wall jets

The velocity measurements were first recorded at initial stations to characterise the flow at bulk flow velocities of 0.120 and 0.252 m/s, which give rise to the momentum thickness Reynolds numbers of 125 and 300, and the Görtler numbers of 10 and 30, respectively.

Spanwise variations of Stanton numbers at the Reynolds number based on the channel width of 4600 ($u=0.12$ m/s) are illustrated in Fig. 15 for four values of the blowing parameter and at three measurement stations. With no blowing, $m=0$, there is a vortex wavelength of around 16 mm which remains constant in the streamwise direction and with an amplitude of 50% of the spanwise averaged Stanton number. With a blowing parameter of 0.4, minimum Stanton numbers appear at 10 mm intervals, equal to the hole spacing but offset in the z direction by 2 mm from the injections hole positions, probably due to the longitudinal offset of the two rows. Towards the end of the curvature section, the effect of the injected flow tends to disappear and the 16 mm wavelength reappears. Again, the amplitude of the spanwise variation of Stanton number is nearly 50% of the spanwise averaged Stanton number. With a blowing parameter of unity, the minimum Stanton numbers are at the same positions as in the previous case with an amplitude of around 40%, probably due to the higher blowing parameter having less influence in the immediate proximity of the wall. With a blowing parameter of 1.5, the 16 mm wavelength occurred with an amplitude of around 30% of the spanwise averaged Stanton

number.

The experimental Stanton numbers may be compared with Eqs. (2) and (3) in Fig. 16, which shows that the spanwise averaged Stanton number increases continuously without injection in the streamwise direction, from just below the constant temperature laminar value at $Re_x=2.47 \times 10^4$ to above

the turbulent value at $Re_x=3.2 \times 10^4$. This result may be compared with that of Crane and Sabzvari⁽¹⁶⁾, who showed that the Stanton number exceeded the analytical flat plate values only after the appearance of inflected velocity profiles and the onset of spanwise meandering of the vortices. While the minimum Stanton numbers remain below Eq. (2), the maximum

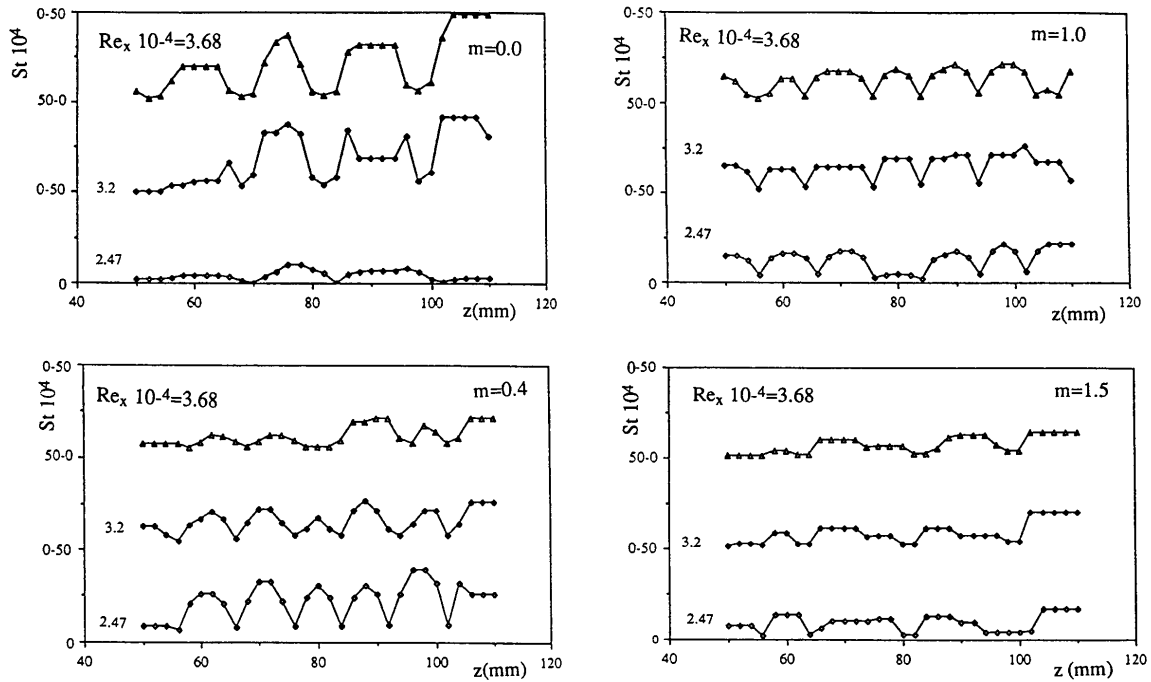


Fig. 15 Spanwise variation of Stanton number at $u=0.120$ m/s

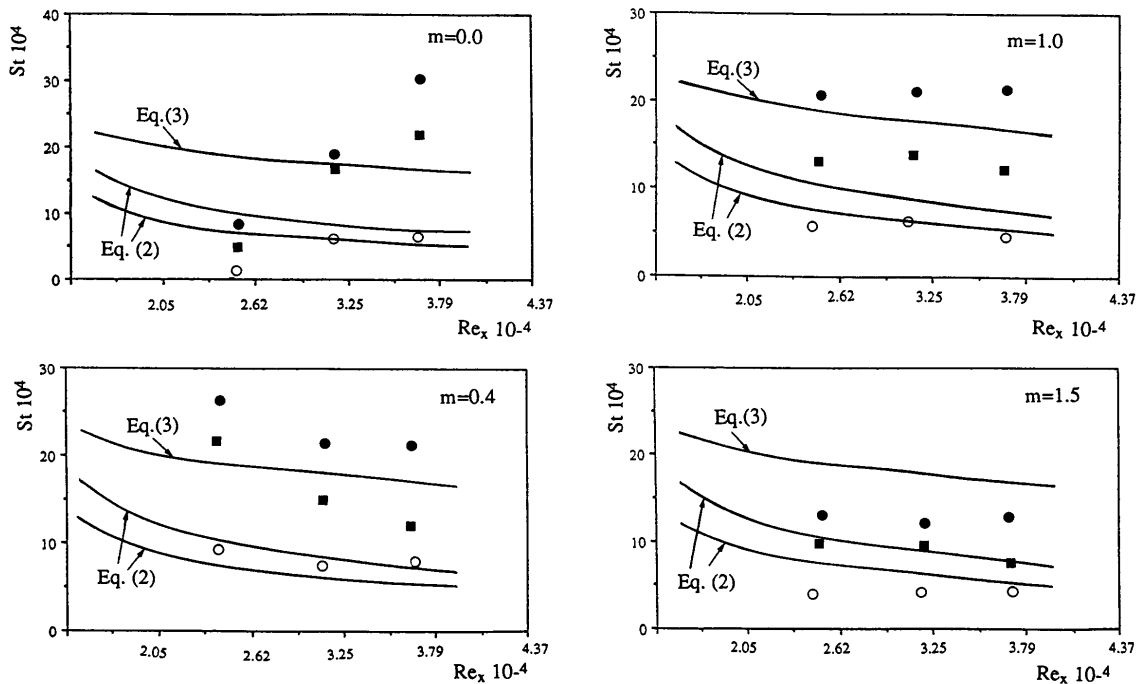


Fig. 16 Experimental Stanton numbers and flat plate correlations at $u=0.120$ m/s ;
 ● : downwash, ○ : upwash, ■ : mean Stanton number

value exceeds Eq. (3) at $Re_x = 3.2 \times 10^4$. With $m = 0.4$, the spanwise-averaged Stanton number decreases with streamwise distance, the minimum Stanton numbers remain close to laminar values, and the maximum Stanton number exceeds turbulent values. With $m = 1$, the spanwise-averaged Stanton number remains above the laminar values, and local values are slightly above the turbulent values at downwash and slightly below the laminar values at upwash; the maximum Stanton numbers are three times larger than those at minimum at all locations. With $m = 1.5$, the streamwise distribution of spanwise averaged Stanton number closely follows the laminar values, and the maximum Stanton numbers exceed the minimum Stanton number by a factor close to three. Then the heat transfer coefficient increases in the streamwise direction in the absence of jets and decreases with discrete hole injection. These results are in partial agreement with those of Ligrani et al.⁽¹⁰⁾, who showed that local Stanton numbers were altered by the vortices and increased more rapidly with downstream distance for $m = 0.47$ than $m = 0.98$.

The spanwise distributions of Stanton number at a Reynolds number based on channel width of 9700 ($u = 0.252$ m/s) with blowing parameters of 0, 0.4, 1.0 and 1.5, are shown in Fig. 17. A more regular vortex system with 16 mm wavelength and an amplitude of around 40% of the spanwise averaged Stanton number occurred along the curvature without injection. Thus, as the flow velocity increased, the vortices became weaker or were unsteady. With a blowing parameter

of 0.4, the amplitude of spanwise variation of Stanton number is around 35% of the spanwise averaged Stanton number and the injected flow has less effect on the vortices than that with $u = 0.120$ m/s. This means that as the flow velocity increases, a higher blowing parameter may be needed for the same spanwise variation. With the blowing parameter of unity, the vortex upwash positions appear at every 10 mm, apparently controlled by the jets with an amplitude of nearly 50% of the spanwise averaged Stanton number, similar to the results with $u = 0.120$ m/s. With the blowing parameter of 1.5, the amplitude of spanwise variation of Stanton number is around 30% of the spanwise averaged Stanton numbers (the same as at $u = 0.120$ m/s for $m = 1.5$).

The maximum, minimum and spanwise averaged Stanton numbers with laminar and turbulent values are shown in Fig. 18. All experimental Stanton numbers decrease in the streamwise direction, unlike the previous case of 0.120 m/s without jets. At $m = 0.4$, the maximum Stanton numbers exceed the minimum values by a factor of more than three, and minimum and spanwise averaged Stanton numbers decrease in the streamwise direction. At $m = 1.0$, the spanwise-averaged and maximum Stanton numbers exceed the minimum values by a factor of more than two and decrease along the downstream of the curvature. At $m = 1.5$, the maximum Stanton numbers exceed those at upwash values by a factor of more than two. The heat transfer coefficient increases as the blowing parameter increases from 0 to 0.4, then decreases

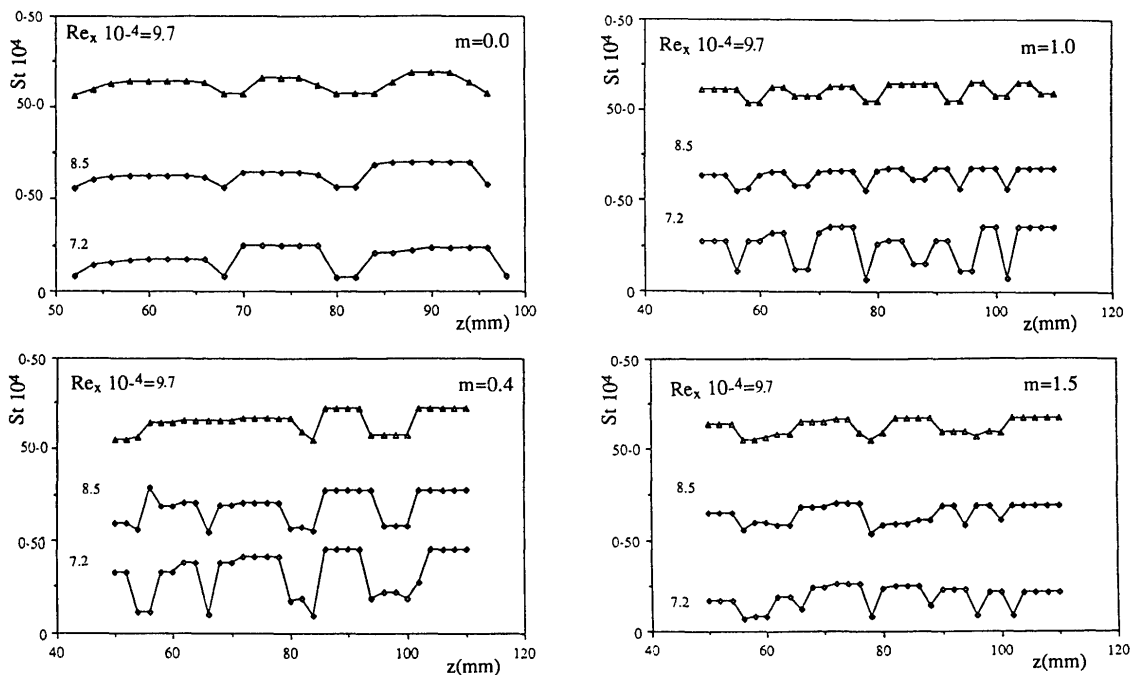


Fig. 17 Spanwise variation of Stanton number at $u = 0.252$ m/s

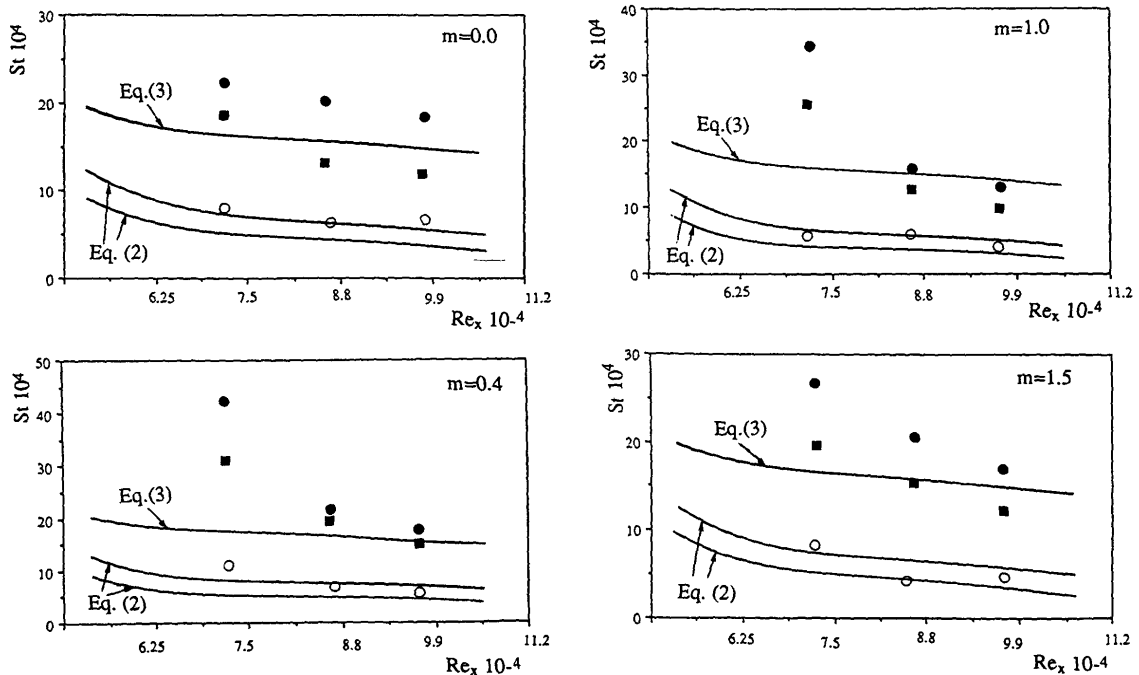


Fig. 18 Experimental Stanton numbers at $u=0.252$ m/s and values for Eqs. (2) and (3); ●: downwash, ○: upwash, ■: mean Stanton number

with increasing m , and the increase in the blowing parameter from 0.4 to 1.5 causes the rate of reduction of spanwise averaged Stanton number to decrease with streamwise distance. The decrease in the heat transfer coefficient for blowing parameters greater than 0.4 is not in agreement with the results of Hartnett et al.⁽⁹⁾, who reported a slight increase with injection flow for the heat transfer coefficient.

4. Conclusions

Measurements of velocity and wall temperature in laminar regions showed that longitudinal vortices were not very strong, and hence vortex generators were used to amplify them. The generators caused stronger and more regular vortex systems to develop and brought about enhancement of the heat transfer coefficient so that the mean Stanton number exceeded the analytical laminar flat plate values by a factor of approximately three. The influence of free stream velocity on longitudinal vortices and heat transfer coefficients with zero pressure gradient was also investigated in transitional/turbulent flows, and it was shown that higher free stream velocities tended to suppress the vortex development so that the heat transfer coefficient increased to 40% above that of flat plates for turbulent boundary layers.

The stabilising effect of favourable pressure gradients together with the destabilising effect of concave curvature was investigated in a range of pressure gradients corresponding to values of up to 1.8×10^{-6} .

It was found that mild pressure gradients which correspond to values of k between 0.2×10^{-6} and 0.75×10^{-6} were conducive to a regular vortex structure and gave rise to an increase in Stanton number, three times larger than that of flat-plate laminar boundary layers while a value of 1.8×10^{-6} , which is smaller than the relaminarisation factor of Launder⁽¹⁸⁾ of 3.2×10^{-6} , suppressed the vortex development so that no augmentation in Stanton number took place above those of the zero pressure gradient.

The influence of discrete wall jets on streamwise vortices and heat transfer coefficients has been determined for a range of blowing parameters up to 1.5 on concave surfaces. For blowing parameters of up to unity, the jets dominated the longitudinal vortices in the near field so that the wavelength remained essentially that of the hole spacing and Stanton numbers initially exceeded those in the absence of wall jets by a factor of more than three. In the far field, streamwise vortices seemed to have reestablished themselves and Stanton numbers decreased. For blowing parameters larger than unity, the jets caused irregularities in the near wall region and after some distance downstream, they interacted with the longitudinal vortices so that the mean Stanton number in the streamwise direction remained almost unchanged. The Stanton number initially increased with a blowing parameter smaller than unity and decreased with unity and higher values.

References

- (1) McCormack, P.D., Welker, H. and Kelleher, M., Taylor-Görtler Vortices and Their Effects on Heat Transfer, *J. Heat Transfer*, Vol. 92, (1979), p. 101.
- (2) Kelleher, M.D., Flentie, D.L. and McKee, R.J., An Experimental Study of the Secondary Flow in a Curved Rectangular Channel, ASME Paper No. 79-FE-6, (1979).
- (3) Kottke, V., Taylor-Görtler Vortices and Their Effect on Heat and Mass Transfer, Proceeding, 8th International Heat Transfer Conference, San Francisco, CA, (1986).
- (4) Crance, R.I. and Umur, H., Concave Wall Laminar Heat Transfer and Görtler Vortex Structure: Effects of Precurvature Boundary Layer and Favourable Pressure Gradients, ASME paper No. 90-GT-94, (1990).
- (5) Thomann, H., Effect of Streamwise Wall Curvature on Heat Transfer on Turbulent Boundary Layer, *J. Fluid Mech.*, Vol. 33, (1968), p. 283.
- (6) Mayle, R.E, Blair, M.I. and Kopper, F. G., Turbulent Boundary Layer Heat Transfer on Curved Surfaces, *J. Heat Transfer*, Vol. 101, (1979), p. 521.
- (7) Simonich, J.C. and Moffat, R.J., Liquid Crystal Visualisation of Surface Heat Transfer on a Concave Curved Turbulent Boundary Layer, *J. Eng. for Gas Turbines and Power*, Vol. 106, (1982), p. 619.
- (8) Gibson, M.M., Verriopoulos, C.A. and Nagano, Y., 1981, Measurement in the Heated Turbulent Boundary Layer on a Mildly Curved Convex Surface, The Symposium on Turbulent Shear Flows, University of California, (1981).
- (9) Hartnett, J.P., Birkebak, R.C. and Eckert, E.R.G., Velocity Distributions, Temperature Distributions, Effectiveness and Heat Transfer for Air Injected through a Tangential Slot into a Turbulent Boundary Layer, *J. Heat Transfer*, Vol. 83, (1961).
- (10) Ligrani, P.M., Ortiz, A., Joseph, S.I. and Evans, D. I., Effects of Embedded Vortices on Film Cooled Turbulent Boundary Layers, ASME paper No. 88-GT-170, (1989).
- (11) Crane, R.I. and Umur, H., 1990, Effects of Accelerating Flow and Discrete Hole Injection on Görtler Vortex Structure, Colloquium on Görtler Vortex Flows, *Euromech 261*, June 11-14, Nantes, France, (1990).
- (12) Umur, H., Flows with Curvature, PhD Thesis, London University, (1991).
- (13) Kays, W.M., Convective Heat and Mass Transfer, (1966), McGraw Hill.
- (14) Kan, S., Miwa, K., Morishita, T., Murakata, Y. and Homura, M., Heat Transfer of a Turbine Blade, Proc. Joint Inst. Gas Turbine Conf., October 1971, Tokyo, (1971).
- (15) Kamotoni, C.Y., Lin, J.K. and Ostrach, S., Effect of Destabilizing Heating on Görtler Vortices, *J. Heat Transfer*, Vol. 107, p. 877, (1985).
- (16) Crane, R.I. and Sabzvari, J., Heat Transfer Visualisation and Measurement in Unstable Concave Wall Laminar Boundary Layers, *Journal of Turbomachinery*, Vol. 111, (1989), p. 51.
- (17) Junkhan, G.H. and Serovy, G.K., Effects of Free Stream Turbulence and Pressure Gradient on Flat Plate Boundary Layer Velocity and on Heat Transfer, *J. Heat Transfer*, Vol. 169, (1967), p. 169.
- (18) Launder, B.E., Laminarization of the Turbulent Boundary Layer in a Severe Acceleration, *J. Appl. Mech.*, Vol. 31, (1964), p. 707.